

Dispersion of Multiwalled Carbon Nanotubes into A Diglyme Solution,

Electrodeposition of Aluminum-Based Composite, and Improvement of

Hardness

Zelei Zhang,^{a,b} Atsushi Kitada,^{b,*} Tianyu Chen,^b Kazuhiro Fukami,^b Masahiro

Shimizu,^{c,d} Susumu Arai,^{c,d} Zhengjun Yao,^a and Kuniaki Murase^b

^a College of Material Science and Technology, Nanjing University of Aeronautics and

Astronautics, Nanjing, 210016, China

^b Department of Materials Science and Engineering, Kyoto University, Kyoto, 606-

8501, Japan

^c Department of Materials Chemistry, Faculty of Engineering, Shinshu University, 4-

17-1 Wakasato, Nagano, Japan

^d Institute of Carbon Science and Technology, Faculty of Engineering, Shinshu

University, 4-17-1 Wakasato, Nagano, Japan

* Corresponding author

E-mail address: kitada.atsushi.3r@kyoto-u.ac.jp (A. Kitada).

Abstract

Composites of metals and carbon nanotubes (CNTs) are of interest due to their better mechanical properties compared to neat materials. Aluminum (Al) composites with multi-walled carbon nanotubes (MWCNTs) have been prepared by room-temperature electrodeposition in a relatively inexpensive and safe organic solvent, i.e. diglyme (G2).

Successful dispersion of MWCNTs in an AlCl_3 -G2 electrodeposition bath was achieved by surface modification i.e. acid treatment of MWCNTs, similar to the case of aqueous baths. Scanning electron microscopy images showed that MWCNTs filled and/or bridged the gap between Al particles, which can be attributed to the high Vickers hardness of 205 ± 14 HV, exceeding 160 HV for Al-MWCNTs obtained by powder metallurgical methods. Additionally, while the Vickers hardness of electroplated Aluminum-CNTs composites has been reported to be 75 HV, an almost three times harder material is reported in the present study.

Keywords: Aluminum; Acid-treated carbon nanotubes; Metal matrix composites;

Electrodeposition; Hardness

1. Introduction

Aluminum (Al) are lightweight materials and have excellent high-temperature corrosion resistance, which belong to an important class of structural materials.^{1,2} Al-based composites with fibers, which fill and/or bridge the gap (or crack) between the matrix, are of interest as damage-tolerant structural materials.³ Multi-walled carbon nanotubes (MWCNTs) possess excellent mechanical properties.^{4,5} Therefore, by introducing MWCNTs, the mechanical properties of Al-based composites have been enhanced.⁶⁻¹³

Because of their intermolecular force (π - π interactions and van der Waals interactions), homogeneous dispersion of MWCNTs in composites has been an issue. Agglomeration of MWCNTs in composites bring adverse effects to composites, that is, the strengthening will be reduced, as they do not provide a three-dimensional network to transfer mechanical loads efficiently.^{8,14} Therefore, the improvement of mechanical properties much depends on the degree of dispersion of the MWCNTs in the Al matrix. The powder metallurgy methods have been predominantly developed to disperse MWCNTs into composites.^{9,10} However, the high-temperature process can form

carbides at interface between metal matrix and MWCNTs, inhibiting interfacial load transfer.¹¹⁻¹³ In addition, to the best of our knowledge, the hardness of Al-MWCNTs obtained by powder metallurgical methods is 40 HV–160 HV.^{9,15-19}

Electrochemical methods are favorable as they are medium- or low-temperature processes which cause less thermal damage to MWCNTs. They have been used to produce metal-MWCNTs composites such as Ni, Ag and Cu, which were electroplated from MWCNTs-dispersed aqueous baths.^{20,21,22} Since Al cannot be electrodeposited from aqueous baths, non-aqueous baths such as organic and ionic liquid baths have been investigated.²³⁻²⁵ However, there has been only one report about electrodeposition of Al–MWCNTs, where an ionic liquid bath was used.²⁶ Although there was no need of the acid treatment to obtain homogeneous dispersion into the bath, the hardness of the Al-MWCNTs composite was as low as 75 HV.²⁶ Therefore, to improve Al–MWCNTs composite plating process, an alternative electrochemical method using safe and inexpensive solvent has been an issue.

In this study, composite electroplating of Al with MWCNTs is studied at room temperature using a diglyme (G2) bath. G2 is an industrially-produced glyme (glycol

ether) material with a high boiling point of 162 °C, and room-temperature Al electrodeposition has been demonstrated from G2 solutions.²⁷⁻³⁰ The preparation process of the Al–MWCNTs involved (i) acid-treatment of MWCNTs for successful dispersion in an AlCl₃–G2 bath using hydrogen-bonding interaction between MWCNTs and G2, and (ii) improvement of the hardness by successful co-electrodeposition of Al with MWCNTs.

2. Experimental

2.1 Acid treatment of carbon nanotubes

By referring some reports,^{14,20,22} the multi-walled carbon nanotubes (MWCNTs) were acid treated with ultrasonication in 3:1 (volume ratio) H₂SO₄ aq (98wt%)/HNO₃ aq (68wt%) for 6 h. The sample was filtered and washed with deionized water until the pH of the filtrate water became neutral. The filtered MWCNTs were dried for 12 h under vacuum at 120°C.

2.2 Characterization of acid-treated MWCNTs

The acid-treated MWCNTs were characterized by Raman spectroscopy (B&W Tek,

innoRam 785) with integration time of 65 s, UV-vis spectroscopy (Hitachi U-3500 equipped with a $\phi 60$ integrating sphere) at a scan rate of 30 nm s^{-1} in 1 mm quartz cuvettes over the wavelength range of 200–800 nm, and X-ray photoelectron spectroscopy (XPS; JEOL, JPS-9010TRX calibrated using the C1s peak at 284.5 eV).

To estimate the Raman intensity, the spectra were fitted by a Lorentzian function (D, G and G' bands) and a Gaussian function (D' band). Acid-treated MWCNTs dispersed in ethanol were dropped on a Cu mesh and characterized by TEM (JEOL, JEM-2100F) to observe their microstructure.

2.3 Bath preparation

All experiments were carried out in an Ar-filled glovebox with O_2 content below 1 ppm. The water content of G2 (diethylene glycol dimethyl ether; Kanto Chemical Co.) was decreased to 35 ppm using molecular sieves (3A, Nacalai Tesque Co.). We added 0.4 g L^{-1} acid-treated MWCNTs to a 1:5 (mole ratio) AlCl_3 -G2 solution, which was then ultrasonicated for 3 h to obtain AlCl_3 -G2 with a dispersion of MWCNTs. Details of the preparation of the AlCl_3 -G2 solution were published elsewhere,²⁸⁻³⁰ while AlCl_3

reagent has been changed to that obtained from Nippon Light Metal Company, Ltd. The as-prepared electrolyte was a brown or yellowish solution due to impurities caused by thermal decomposition during the addition of AlCl_3 . For purification pre-electrolysis was conducted for more than 24 h at a potential of -1 V vs. Al quasi reference electrode (QRE) using Cu working electrode and Al counter electrode until the solution became colorless and the electrodeposits covered the entire immersed area of the Cu working electrode. No additives were mixed into the AlCl_3 -G2 solution.

2.4 Electrochemical measurements

All electrochemical measurements were performed at room temperature in an Ar-filled glovebox using a VSP-300 multichannel potentiostat/galvanostat (Bio-Logic Science Instruments SAS) with a conventional three-electrode configuration in a glass cell at room temperature. Cu sheet (0.2 mm in thickness) was used as a working electrode (WE) and Al sheets (0.5 mm in thickness) were used as the counter electrode (CE) and quasi reference electrode (QRE). All electrodes were cleaned using acetone for 20 min and then ethanol for 20 min before electrochemical measurements. Cyclic

voltammetry (CV) for the electrolyte with MWCNTs was carried out between -1 V and $+1$ V vs. Al QRE at a scan rate of 20 mV s $^{-1}$.

Electrodeposition was conducted on Cu WE at room temperature without agitation using potentiostatic electrodeposition at -1.5 V vs. Al QRE. After electrodeposition, the electrodeposits were rinsed with neat G2 twice to remove the residual AlCl $_3$ -G2 solution and MWCNTs on the surface.

2.5 Characterization of Al and Al-MWCNTs electrodeposits

The Al electrodeposits with and without MWCNTs were characterized by X-ray diffraction (XRD) and scanning electron microscopy (SEM). XRD profiles were obtained using a Rigaku RINT2200 with Cu $K\alpha$ radiation at a scan rate of 0.3° min $^{-1}$. SEM observations were conducted using Keyence VE-8800 system with the accelerating voltage of 20 kV and energy dispersive X-ray (EDX) spectrometry was performed using EDAX VE-9800. The micro-Vickers hardness of Al and Al-MWCNTs deposits was determined by the micro-hardness tester (Mitutoyo, HM-200) with a load of 196.1 mN.

3. Results and discussion

3.1 Effect of acid treatment on the MWCNTs

Figure 1 shows the Raman spectra measured from 1000 to 3000 cm^{-1} of as-received and acid-treated MWCNTs, which showed different intensities of the D, D', G and G' bands. The G band (1577 cm^{-1} or 1580 cm^{-1}) and G' band (2617 cm^{-1}) correspond to the stretching mode of the C-C bond in the sp^2 carbon network, while the D band and D' band are related to defects in the sp^2 carbon network.^{13,31,32} The intensity ratio of the D and G bands (I_D/I_G) was sensitive to variations in the structural defects of MWCNTs after acid treatment in the $\text{H}_2\text{SO}_4/\text{HNO}_3$ solution.³³ The as-received MWCNTs showed a value of $I_D/I_G = 0.30$ (Fig. 1a), which increased to $I_D/I_G = 1.05$ after acid treatment (Fig. 1b), proving that the defects were introduced by acid treatment.

To investigate the defects or functional groups of the acid-treated MWCNTs, XPS measurements were performed. As shown in Fig. 2, the C1s peak of the acid-treated MWCNTs was fitted by six synthetic peaks. Consequently, the C-O, C=O, and -COO- groups, indicated by the dotted lines in Fig. 2, were introduced. As shown in the inset

of Fig. 2, the diameter of the MWCNTs was over 100 nm and their side walls were damaged by the acid treatment, indicating that the functional groups may have been located on the side-wall defects of the MWCNTs.³¹

3.2 Dispersion of acid-treated MWCNTs into G2

For checking the dispersion state, we measured the mixture of acid-treated MWCNTs into G2 without AlCl_3 , since it was difficult to measure the hygroscopic AlCl_3 -G2 solution in air despite the use of a screw-capped quartz cell.

Figure 3a shows the UV-vis absorption spectra for acid-treated MWCNTs in G2 solution with and without ultrasonication for 3 h. The pure G2 was used as the reference sample. The presence of the absorption peak below 330 nm verified that the individual MWCNTs can be dispersed in the G2 solution with ultrasonication, while the peak is caused by plasmon resonance of π electrons of free MWCNTs and its shape is related to the size distribution of MWCNTs.^{14,34,35} In contrast, the bundled MWCNTs (without ultrasonication) showed no absorption change in this region. Notably, without acid-treatment, the MWCNTs could not be dispersed in G2 even with sonication, due to

strong intermolecular interactions of MWCNTs. Thus, hydrogen bonds are formed between the carboxyl/hydroxyl groups of acid-treated MWCNTs and the oxygen atoms of G2, and they are essential for the dispersion. By contrast, for the Al–MWCNTs composite plating from an imidazolium-based ionic liquid, the π - π interaction between CNTs and solvent (ionic liquid) is necessary for uniform distribution in the plating bath.²⁶ Consequently, the introduction of hydrogen bonds between the MWCNTs and G2 can prevent re-aggregation of MWCNTs, consistent with the absorption intensity being maintained for 6 h (see [Fig. 3c](#)). It is also notable that in the case of aqueous solutions, the acid-treatment is also effective for homogeneous dispersion of MWCNTs.²⁰⁻²²

3.3 Electrochemical measurements

[Figure 4a](#) shows the CVs for Al-MWCNTs (red curves; referred to as “with MWCNTs”) and neat Al (black curves; without MWCNTs). The MWCNTs showed a clear influence on the CV curve of AlCl_3 -G2, that is an increase in deposition overpotential. At the initial stage of electrodeposition, some of MWCNTs could be

adsorbed on Cu WE. Therefore, the increased deposition overpotential for “with MWCNTs” may indicate that electrodeposition of Al on the MWCNTs is more difficult than that of Al on Cu WE, although MWCNTs have good electrical conductivity.⁵

Figure 4b displays the cathodic current-time plots for Al electrodeposition from AlCl₃-G2 solution with and without MWCNTs. During the double layer charging, the cathodic current density initially increased suddenly and drops to a minimum in a short period of time, followed by a nearly constant value of ca. 11 mA cm⁻² for with MWCNTs and ca. 12 mA cm⁻² for neat Al (without MWCNTs), which indicates that the deposits maintain an almost constant surface area during electrodeposition.

3.4 Crystallographic and morphology features of the deposits coating

Figure 5 shows the XRD profiles of the Al electrodeposits with and without MWCNTs on Cu substrates obtained at -1.5 V, showing no impurities such as Al₂O₃. Since there was no significant change in the full width at half maximum, the relative intensities of XRD peaks depend on the preferential orientation. The Al and Al-MWCNTs grew preferentially along the <111> direction, and the intensity ratio of the

111 and 220 peaks (I_{111} / I_{220}) was 4.15 for neat Al and 3.07 for Al–MWCNTs, while the standard intensity ratio (I_{111} / I_{220}) is 2.09. Moreover, the peak intensity ratio of Al–MWCNTs was less than that of neat Al, implying that MWCNTs as a second-phase particle suppressed the anisotropy of crystal growth. Pangarov reported that, when the current density (per efficient surface area) is larger (i.e. if the overpotential from the equilibrium is larger), deposits will be $\langle 111 \rangle$ oriented in the case of fcc metal such as Al.³⁶ The efficient surface area was nearly constant in both deposits since the cathodic current density became almost constant (see Fig. 4b). Thus, the smaller cathodic current density of Al–MWCNTs can also explain the smaller anisotropy.

Figure 6 shows SEM images of the top surface of Al (Figs. 6a and 6b) and Al–MWCNTs (Fig. 6c and 6d). The deposits had a flake-like morphology, and the electrodeposition from the AlCl_3 –G2–MWCNTs solution gave thinner flake-like deposits. In the top view of the Al–MWCNTs composites, only a few MWCNTs were observed (shown by dashed circle and oval), as most of the MWCNTs may be coated by Al electrodeposits or may be washed out after rinsing by neat G2. In contrast to Fig. 6, MWCNTs can be observed at the fracture surface of the Al–MWCNTs composites

(see Fig. 7). We observed many MWCNTs at two different local areas. The observed MWCNTs in the composites had two characteristic morphologies, that is parallel and bridging manner. The monodispersed MWCNTs (marked with arrows) and a few multi-dispersed but not heavily entangled MWCNTs (marked by oval), were embedded into Al deposits. Notably, the degree of agglomeration is much lower than that for non-acid-treated MWCNTs in electrodeposited Al matrix.²⁶ Some of the MWCNTs (marked with red arrows and lines) were aligned parallel to the flake-like Al particles, while the other MWCNTs (marked with green arrows and lines) were bonded almost vertically to a few adjacent Al particles, in a bridging manner. The enlarged SEM images are shown in Fig. 8, both for parallel manner (Figs. 8a and 8b) and bridging manner (Figs. 8c and 8d).

3.5 Vickers hardness and effects of impurities

It has been reported that, using powder metallurgical methods, the hardness of Al–CNTs composites ranges between 40 HV and 160 HV,^{9,15-19} while the hardness is 22–30 HV for non-electrodeposited, commercial-purity Al without plastic deformation processing.^{9,37,38} It is also reported that the electrodeposited Al shows the hardness of

at most 1.7 GPa or 170 HV.^{38,39} Figure 9 shows the results of Vickers test for the electrodeposited Al and Al-MWCNTs samples. Surprisingly, the Vickers hardness of the Al-MWCNTs composite obtained from the AlCl₃-G2 bath was as high as 205±14 HV or 2.01±0.14 GPa. The value is approximately 24% larger than that of the neat Al deposits (165±17 HV or 1.62±0.17 GPa), and almost three times stronger than Al-CNTs (75 HV) deposited from ionic liquid.²⁶

The reason why the hardness improved is that MWCNTs fill and/or bridge the gap between the Al particles in the composites. And the increase of hardness is also attributed to the homogeneous dispersion of MWCNTs in Al-MWCNTs composite coating. It is possible that agglomeration of “non-acid-treated MWCNTs” is inevitable because of van der Waals or π - π interaction between MWCNTs, giving lower hardness for previous report.²⁶ By contrast, the acid-treated MWCNTs with the weakened π - π interaction resulted in higher hardness due to less agglomeration. It is also notable that the side-wall defects of acid-treated MWCNTs did not bring adverse effect on the mechanical property.

The impurities incorporated from electrodeposition baths can increase the hardness of Al.³⁸⁻⁴⁰ Different from the case of dimethylsulfone (DMSO₂)-based Al electrodeposition baths, where S, Cl and C can be incorporated, the main impurity for the glyme bath is only Cl and C. The contents were estimated by SEM-EDX analysis for some local areas of Fig. 9, that is polished cross-section of the electrodeposits. The Cl content was 0.7 at% and C content was 0.4–0.5 at%, both for neat Al and Al-MWCNTs. Thus, the concentration of MWCNTs in the composites could not be determined. However, the similarity of the total contents of Cl and C clearly demonstrate that the microhardness is improved by the incorporation of the MWCNTs, even though the amount is less than 0.5 at%. It is unlikely that grain size effects caused the improvement of the hardness between neat Al and Al-MWCNTs, because the FWHM of XRD peaks in Fig. 5 were very similar.

The XRD profiles in Fig. 5 also clarified that the <111> preferential orientation is relatively weak in the case of G2 bath compared to the case of DMSO₂ baths. While the total impurity content (S, Cl, and Ga for DMSO₂, Cl for G2) is almost the same (0.7 at%), 200 and/or 220 intensities are very weak when non-Cl elements such as S and Ga

were incorporated.³⁸⁻⁴⁰ It has been considered that the weakened 200 and/or 220 intensities are due to growth inhibition by impurity elements including Cl. From our results, however, Cl has much weaker effect on growth inhibition than S and Ga.

4. Conclusion

An alternative approach to obtain hard Al–MWCNTs composites is provided using a G2 electrodeposition bath. Like in the aqueous baths, the acid-treated MWCNTs achieved a good dispersion in AlCl₃–G2 solution due to hydrogen bonding between G2 and carboxyl/hydroxyl groups of MWCNTs. We consider it crucial to the homogeneous dispersion of MWCNTs in the composite structure. Notably, in spite of the low concentration of MWCNTs in the glyme-AlCl₃ solution (0.4 g L⁻¹), the electrochemical behaviors of the plating bath and the characteristics of electrodeposits have been influenced. Also, the incorporation of MWCNTs into Al matrix raised the hardness by 24%. In addition, the effect of Cl on growth inhibition of Al electrodeposits are weak compared to S and Ga.

Acknowledgments

This work was supported financially by Grants-in-Aid for Scientific Research (B) (No. 19H02490: A. K.) from the Japan Society for the Promotion of Science (JSPS). A. K. thanks Iketani Science and Technology Foundation (0311028-A) for their financial supports. Z. Z. was financially supported by the China Scholarship Council (CSC), and the Project Funded by the Priority Academic Program Development of Jiangsu Higher Education Institutions. The authors declare no competing interests.

References

1. J. C. Williams and E. A. Starke, *Acta Mater.*, **51**, 5775 (2003).
2. J. Hirsch and T. Al-Samman, *Acta Mater.*, **61**, 818 (2013).
3. R. O. Ritchie, *Nat. Mater.*, **10**, 817 (2011).
4. M. F. Yu, O. Lourie, M. J. Dyer, K. Moloni, T. F. Kelly and R. S. Ruoff, *Science*, **287**, 637 (2000).
5. M. F. L. De Volder, S. H. Tawfick, R. H. Baughman and A. J. Hart, *Science*, **339**, 535 (2013).
6. S. R. Bakshi, D. Lahiri and A. Agarwal, *Int. Mater. Rev.*, **55**, 41 (2010).
7. J. G. Park, D. H. Keum and Y. H. Lee, *Carbon*, **95**, 690 (2015).
8. S. R. Bakshi and A. Agarwal, *Carbon*, **49**, 533 (2011).
9. H. Kwon, M. Estili, K. Takagi, T. Miyazaki and A. Kawasaki, *Carbon*, **47**, 570 (2009).
10. C. F. Deng, X. X. Zhang, D. Z. Wang, Q. Lin and A. B. Li, *Mater. Lett.*, **61**, 1725 (2007).
11. A. D. Moghadam, E. Omrani, P. L. Menezes and P. K. Rohatgi, *Composites Part B*, **77**, 402 (2015).
12. S. C. Tjong, *Mater. Sci. Eng., R*, **74**, 281 (2013).
13. B. A. Chen, S. F. Li, H. Imai, L. Jia, J. Umeda, M. Takahashi and K. Kondoh, *Mater. Des.*, **72**,

- 1 (2015).
14. Y. Wang, J. Wu and F. Wei, *Carbon*, **41**, 2939 (2003).
 15. S. Simoes, F. Viana, M. A. L. Reis and M. F. Vieira, *Metals*, **7**, 279 (2017).
 16. Y. F. Wu and G. Y. Kim, *J. Mater. Process. Technol.*, **211**, 1341 (2011).
 17. T. Tokunaga, K. Kaneko and Z. Horita, *Mater. Sci. Eng., A*, **490**, 300 (2008).
 18. D. D. Phuong, P. V. Trinh, N. V. An, N. V. Luan, P. N. Minh, R. K. Khisamov, K. S. Nazarov, L. R. Zubairov, R. R. Mulyukov and A. A. Nazarov, *J. Alloys Compd.*, **613**, 68 (2014).
 19. F. Ostovan, K. A. Matori, M. Toozandehjani, A. Oskoueian, H. M. Yusoff, R. Yunus and A. H. M. Ariff, *Materials*, **9**, 140 (2016).
 20. S. Arai and J. Fujii, *J. Electrochem. Soc.*, **158**, D506 (2011).
 21. Ji K, Zhao H, Zhang J, Chen J, Dai Z, *Appl. Surf. Sci.*, **311**, 351 (2014).
 22. S. Arai, M. Ozawa and M. Shimizu, *J. Electrochem. Soc.*, **163**, D774 (2016).
 23. Y. Zhao and T. J. VanderNoot, *Electrochim. Acta*, **42**, 3 (1997).
 24. S. K. Das, S. Mahapatra and H. Lahan, *J. Mater. Chem. A*, **5**, 6347 (2017).
 25. T. Tsuda, G. R. Stafford, and C. L. Hussey, *J. Electrochem. Soc.*, **164**, H5007 (2017).
 26. N. Yatsushiro, N. Koura, S. Nakano, K. Ui and K. Takeuchi, *Electrochemistry*, **74**, 233 (2006).
 27. L. D. Reed, A. Arteaga, and E. J. Menke, *J. Phys. Chem. B*, **119**, 12677 (2015).
 28. A. Kitada, K. Nakamura, K. Fukami and K. Murase, *Electrochim. Acta*, **211**, 561 (2016).
 29. A. Kitada, K. Nakamura, K. Fukami and K. Murase, *Electrochemistry*, **82**, 946 (2014).
 30. A. Kitada, K. Nakamura, K. Fukami and K. Murase, *J. Surf. Finish. Soc. Jpn.*, **69**, 310 (2018).
 31. S. Osswald, M. Havel and Y. Gogotsi, *J. Raman Spectrosc.*, **38**, 728 (2007).
 32. L. Bokobza and J. Zhang, *eXPRESS Polym. Lett.*, **6**, 601 (2012).
 33. M. S. Dresselhaus, A. Jorio, M. Hofmann, G. Dresselhaus and R. Saito, *Nano Lett.*, **10**, 751 (2010).
 34. Y. Ye, S. J. Cai, M. Yan, T. Y. Chen and T. L. Guo, *Appl. Surf. Sci.*, **284**, 107 (2013).
 35. R. Rastogi, R. Kaushal, S. K. Tripathi, A. L. Sharma, I. Kaur and L. M. Bharadwaj, *J. Colloid Interface Sci.*, **328**, 421 (2008).
 36. N. A. Pangarov, *J. Electroanal. Chem.*, **9**, 70 (1965).
 37. S. N. Alhajeri, N. Gao, T. G. Langdon, *Mater. Sci. Eng., A* **528**(10-11) 3833 (2011).
 38. M. Miyake, H. Motonami, S. Shiomi and T. Hirato, *Surf. Coat. Technol.*, **206**, 4225 (2012).
 39. I. Matsui, Y. Hanaoka, S. Ono, Y. Takigawa, T. Uesugi, K. Higashi, *Mater. Lett.*, **109**, 229 (2013).

40. C. Kuma, K. Sato, Y. Hanaoka, I. Matsui, Y. Takigawa, T. Uesugi and K. Higashi, *J. Alloys Compd.*, **783**, 919 (2019).

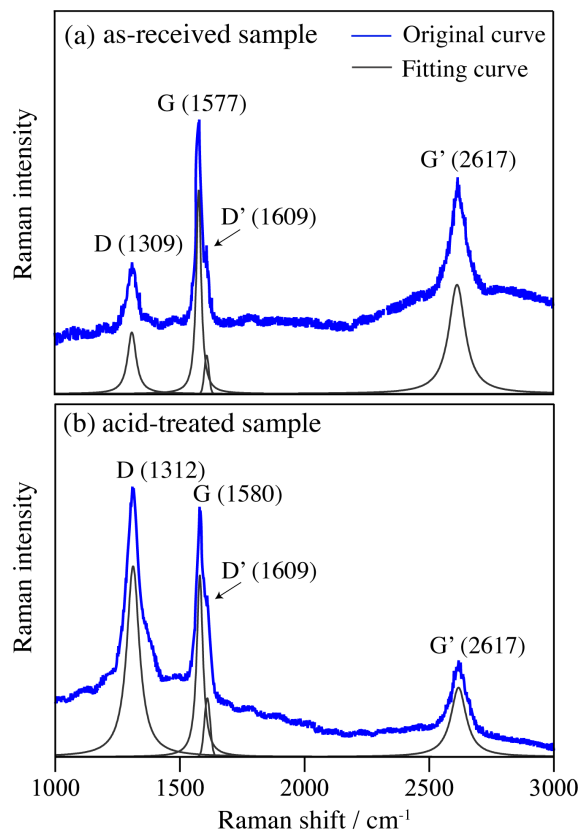


Figure 1 Raman spectra of MWCNTs: (a) as-received sample and (b) acid-treated sample.

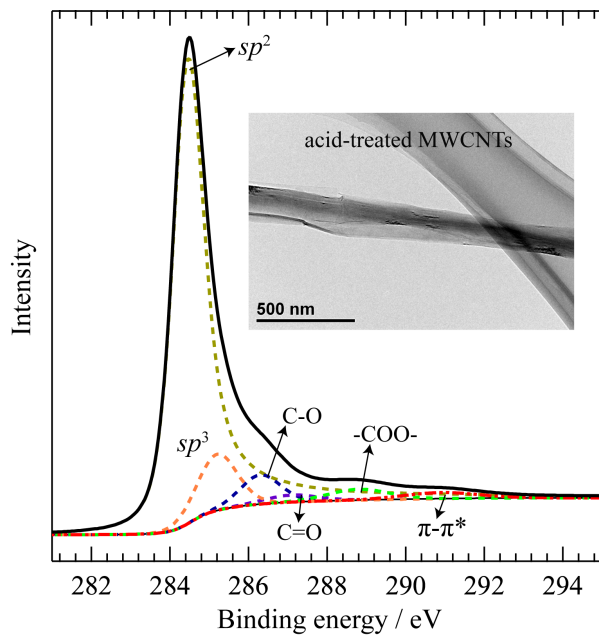


Figure 2 C1s XPS spectra and TEM micrographs of acid-treated MWCNTs.

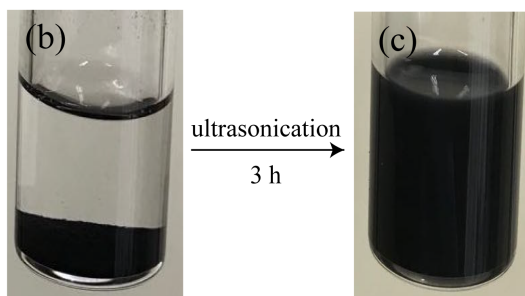
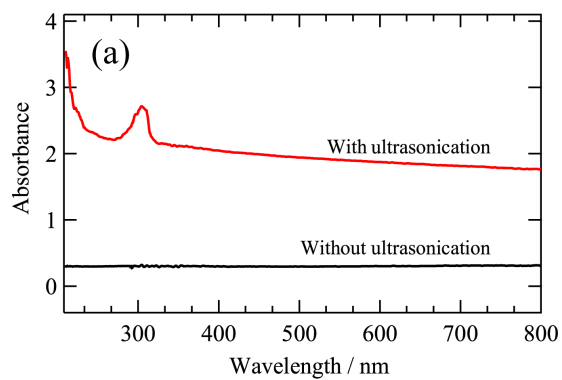


Figure 3 (a) UV-vis absorption spectra of MWCNTs in G2 solution with and without ultrasonication and (b)-(c) photographs of the dispersity of MWCNTs in AlCl₃-G2 before and after ultrasonication for 3 h.

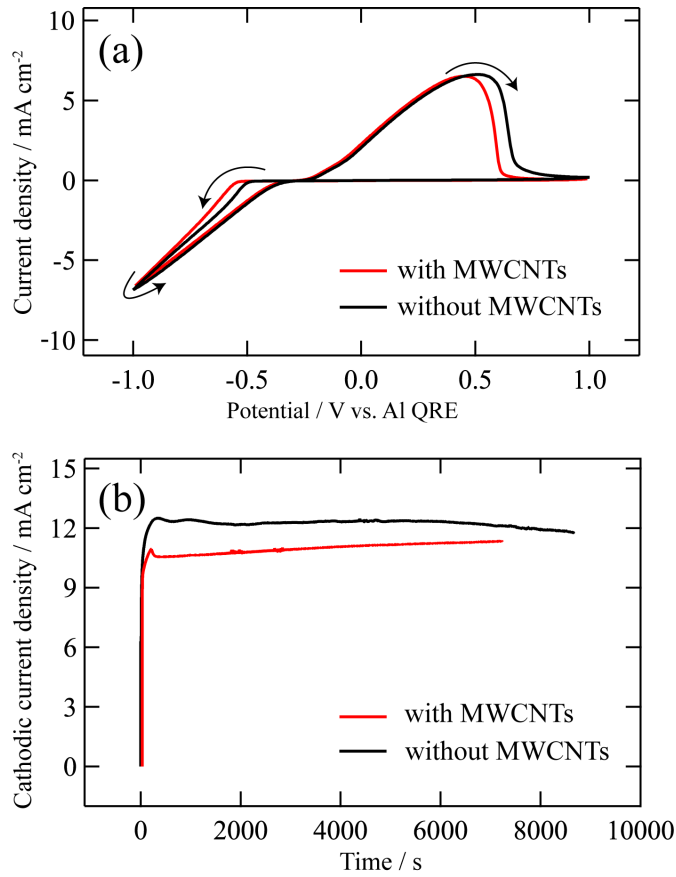


Figure 4 (a) Typical cyclic voltammogram and (b) cathodic current-time plots for potentiostatic electrodeposition at -1.5 V vs. Al QRE from AlCl_3 -G2 solution with and without MWCNTs.

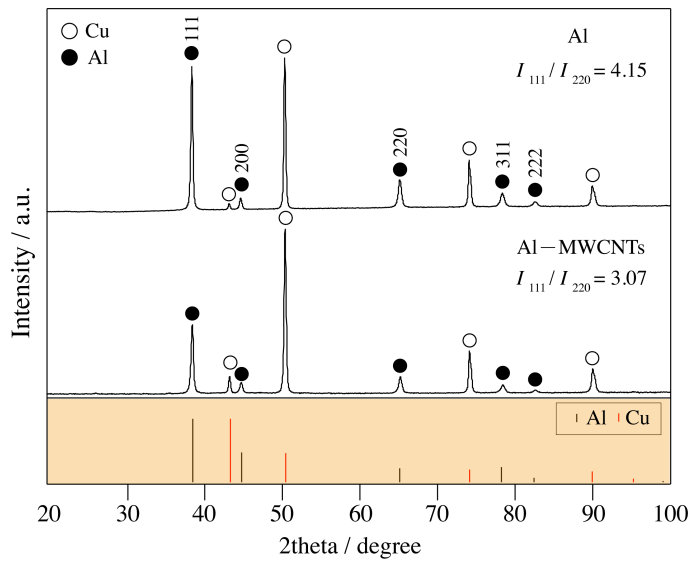


Figure 5 XRD profiles of electrodeposited Al and Al-MWCNTs, with noting ratio of 111 peak intensity over 220 peak intensity, I_{111}/I_{220} , and standard XRD profiles of Al (PDF card 01-071-4625) and Cu (PDF card 00-004-0836).

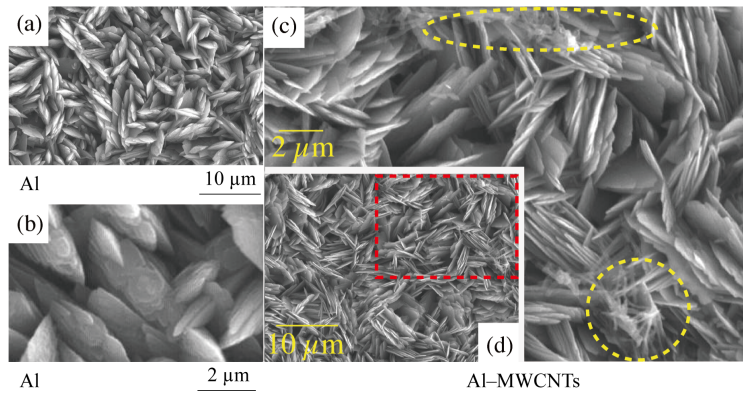


Figure 6 SEM images in plan view of (a)-(b) Al and (c)-(d) Al-MWCNTs deposits, where MWCNTs are marked by yellow dashed circle and oval; (d) shows the whole area and the enlarged area is indicated by red dashed box.

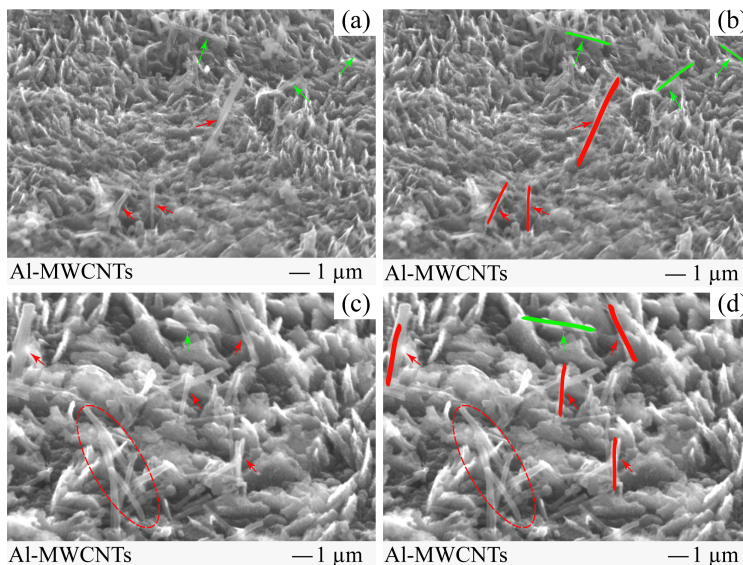


Figure 7 SEM images of fracture surface of Al-MWCNTs deposits: (a) Al with individual MWCNTs, which are emphasized as red and green lines in (b); (c) Al with agglomerate MWCNTs (red oval) and individual MWCNTs (emphasized as red and green in (d)).

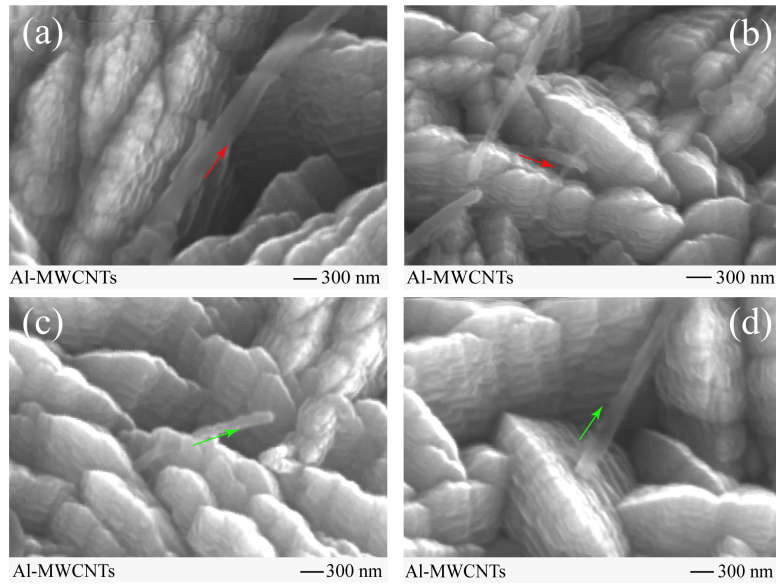


Figure 8 The enlarged view of fracture surface of Al-MWCNTs deposits: (a)-(b)

MWCNTs in a parallel manner and (c)-(d) MWCNTs in a bridging manner.


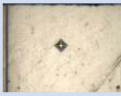
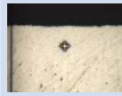

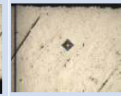





Vickers test	$n = 1$	$n = 2$	$n = 3$	$n = 4$	$n = 5$
Al					
165±17 HV	152.9 HV	157.4 HV	185.6 HV	149.2 HV	181.5 HV
Al-MWCNTs					
205±14 HV	197.0 HV	200.7 HV	187.3 HV	219.9 HV	217.7 HV

Figure 9 Results of Vickers test for electrodeposited Al and Al-MWCNTs, listing average values of Vickers hardness and data set with their optical microscope images.